Received: 28 March 2019 | Revised: 15 July 2019 | Accepted: 12 August 2019

DOI: 10.1002/fsn3.1203

ORIGINAL RESEARCH

Food Science & Nutrition Open Access WILEY

Effect of superfine grinding on the physicochemical properties of bulbs of *Fritillaria unibracteata* Hsiao et K.C. Hsia powder

Cai-xia Li[1,2] | Ying-ying Liu[1,2] | Hai-sheng Feng[1,2] | Shi-zhen Ma[1,2]

[1]Northwest Institute of Plateau Biology, Chinese Academy of Sciences, Xining, China

[2]Qinghai Provincial Key Laboratory of Qinghai-Tibet Plateau Biological Resources, Xining, China

Correspondence
Shi-zhen Ma, Northwest Institute of Plateau Biology, Chinese Academy of Sciences, Xining, Qinghai 810008, China.
Email: szma@nwipb.cas.cn

Funding information
Natural Science Foundation of Qinghai Province for Young Scholars, Grant/Award Number: 2016-ZJ-958Q; Development Project of Qinghai Provincial Key Laboratory, Grant/Award Number: 2017-ZJ-Y10; Capacity Building Project of Engineering Research Center of Qinghai Province, Grant/Award Number: 2017-GX-G03

Abstract

This work aimed to determine the influence of superfine grinding on the physicochemical properties of bulbs of *Fritillaria unibracteata* Hsiao et K.C. Hsia (BFU) powder. For this purpose, fine powder (FP) and two superfine powders (SPs) were obtained via superfine and conventional grinding methods. The properties of different powders were studied and compared. Compared with FP, SPs exhibited higher values in terms of the angle of repose, swelling capacity, ethanol extraction yield, total alkaloid content, and imperialine content, while lower values in terms of particle size and bulk density. Especially, the total alkaloid content of SP-I increased by 66.7%. Proper grinding is more conducive to reduce particle size and improve alkaloid content. FTIR analysis indicates that no new functional groups produced after superfine grinding. XRD analysis suggests that grinding treatment lead to decreases in the crystallinity. Therefore, superfine grinding displays immense potential in the BFU application.

KEYWORDS

Fritillaria unibracteata, particle size, powder, property, superfine grinding

1 | INTRODUCTION

Bulbs of *Fritillaria unibracteata* Hsiao et K.C. Hsia (BFU) is a valuable health food and a well-known traditional Chinese herb (State Pharmacopoeia Committee, 2015a). Specifically, BFU is mainly used to ease coughing and remove phlegm and is considered to exhibit more positive effects relative to other *Fritillaria* species (Zhou et al., 2017). Alkaloids were considered as the active ingredients of BFU that significantly inhibit cough frequency (Hao, Gu, Xiao, & Peng, 2013). Starch is the main component in BFU and accounts for approximately 70%–80% of the total biomass of *Fritillaria* (Gao, Fan, & Paek, 1999). Given that BFU are mainly obtained from its wild species, excessive harvesting of the plants has led to a decline in the species (Li, Dai, & Chen, 2009). Furthermore, increasing market demands resulted in the surging prices of BFU, thereby augmenting its overexploitation and exacerbating its scarcity (Li et al., 2013). Thus, it is necessary to explore an effective utilization method to increase bioavailability and saving BFU resources.

Superfine grinding technology is a useful technology to fabricate superfine powder with changed surface properties and leads to excellent characteristics that are absent in conventional powders (Zhang, Zhang, & Shrestha, 2005). Extant studies report on the superfine grinding of a few foods and traditional Chinese medicinal materials (Chen, Ai, & Huang, 2014; Tao et al., 2014; Xiao, Zhang, Fan, & Han, 2017). The decrease in powder particle size with superfine grinding increases the particle surface area and the breakdown of cell walls, increases particle extraction, and improves particle activity (Zhao et al., 2014, 2010). Thus, superfine grinding is potentially a good method to improve food material bioavailability and bioactivity. However, there is a paucity of information on the effects of superfine grinding on the physicochemical properties of BFU powder.

The aim of the present study involves investigating the application of superfine grinding technology on BFU powders. To accomplish this, BFU powders with different sizes were manufactured. Additionally, we investigated the effects of superfine grinding on the BFU powder

properties including particle size distribution, morphology, angle of repose, bulk density, moisture absorption, swelling capacity, ethanol extraction yield, total alkaloid content, and the contents of isosteroidal alkaloids (peimissine, verticine, verticinone, and imperialine). Fourier transform infrared (FTIR) spectroscopy and X-ray diffraction (XRD) characterizations of different BFU powders were also compared.

2 | MATERIALS AND METHODS

2.1 | Materials

Dry BFU were collected from Songpan County of Sichuan Province in October 2016, and stored at 4°C. Sipeimine standard (HPLC ≥ 98%) was procured from Beijing Solaibao Technology Co. LTD. Peimissine, verticine, verticinone, and imperialine standards were purchased from National Institutes for Food and Drug Control. HPLC grade solvents including methanol and acetonitrile were purchased from XinLanJing International Corporation. All other chemical reagents were purchased locally and were of analytical grade.

2.2 | Sample preparation

2.2.1 | Fine powder

The BFU were set in an oven (DHG-9070A) at 40°C for 4 hr. Subsequently, the dried BFU was subjected to conventional grinding using a high-speed multi-function grinder (SL-500A) for 30 s. The type of milling was knife mill. The crushing time was 30 s, and the motor rated speed was 29344 *g*. The prepared powder was termed as BFU fine powder (FP).

2.2.2 | Superfine powder

A certain amount of FP (5.00 g in each tank) was placed into a vertical planetary ball mill (MITR-TRXQM-0.4L; Changsha Miqi Instrument Equipment Co., Ltd). The grinding tank was composed of agate and exhibited a capacity of 100 ml. The agate grinding balls with different diameters (Φ5, Φ8, and Φ10, mm) were used. Superfine powder I (SP-I) was ground under the following conditions: grinding time corresponding to 1 hr, the weight ratio of ball to material corresponding to 12:1, and rotating speed corresponding to 6 *g*. Superfine powder II (SP-II) was ground under the following conditions: grinding time corresponding to 3 hr, the weight ratio of ball to material corresponding to 20:1, and rotating speed corresponding to 12 *g*.

2.3 | Particle size measurements

The particle size distribution was measured using a Mastersizer 2000 (Malvern Instruments, Malvern) at room temperature. Approximately 0.1 g of powder was dispersed in 10 ml of ultrapure water and shaken on a vortex shaker (DL-SC05, Beijing Donglinchangsheng Biotechnology Co., Ltd) until the sample was fully homogeneous. The obtained suspension was added dropwise to the sample area containing approximately 800 ml of ultrapure water until the range of light obscuration was between 10% and 20%. Stirring speed of dispersion unit was kept at 1,800 rpm. A general-purpose analysis model was used with particle refractive and absorption indices of 1.520 and 0.1, respectively, while the refractive index of water was 1.330. Particle size distribution was characterized via D_{90} and the span value $[(D_{90} - D_{10})/D_{50}]$ wherein D_{10}, D_{50}, and D_{90} values represent 10%, 50%, and 90%, respectively, cumulative volume percentiles of particles with diameters smaller than the value. Three measurements were performed for each sample.

2.4 | Scanning electron microscope (SEM)

The BFU powder samples were spread on a conductive adhesive carbon tape that was pasted on a sample stub. The morphological characteristics of different powder samples were investigated using a SU8010 field emission scanning electron microscope (SEM; Hitachi).

2.5 | Moisture absorption

Based on drug moisture absorption test guidelines in Pharmacopoeia (State Pharmacopoeia Committee, 2015b), the moisture absorptions of different BFU powders were determined.

2.6 | Angle of repose and bulk density

The angle of repose and bulk density of BFU powders were measured using appropriate methods previously validated by Zhao, Yang, Gai, and Yang (2009).

The bulk density (g/ml) was the density including pores and interparticle voids. Three types of BFU powders were filled in a 10-ml volumetric flask (M_1) up to the mark and were weighed (M_2) separately. The bulk density of BFU powder was calculated as follows:

$$\text{Bulk density} = (M_2 - M_1)/10.$$

where M_2 was the total weight of the BFU powder and flask, and M_1 was the weight of the flask only. The measurement of each sample was repeated five times.

The angle of repose was measured using the following steps. Firstly, one filler was fixed above graph paper so that the distance of the paper from the outlet of the filler (H) was 3 cm, and the filler was vertical to the paper. Then, the BFU powder was poured into the filler until the tip of the powder cone touched the outlet of the filler. The diameter ($2R$) of the cone was measured for each powder. The angle of repose (θ) was calculated as the following formula:

$$\theta = \text{arctg}\,(2R/H).$$

where R was the radius of the cone formed by the BFU powder, and H was the distance from the paper to the outlet of the filler. The measurement of each sample was repeated five times.

TABLE 1 Particle sizes of BFU powders (Mean ± *SD*, *n* = 3)

	D_{10} (μm)	D_{50} (μm)	D_{90} (μm)	Span value
FP	13.85 ± 0.12b	30.78 ± 0.50b	271.95 ± 15.12c	8.38 ± 0.35c
SP-I	11.26 ± 0.17a	25.69 ± 0.13a	45.15 ± 0.22a	1.32 ± 0.01a
SP-II	16.00 ± 0.19c	42.34 ± 1.03c	154.02 ± 30.54b	3.25 ± 0.64b

Note: Different lowercase letters in the same column indicate significant difference among the different treatments at the 0.05 level.

2.7 | Swelling capacity

The swelling capacities of different BFU powders were measured by the determination method of swelling capacity in Pharmacopoeia (State Pharmacopoeia Committee, 2015b).

2.8 | Determination of ethanol extraction yield

Based on the extract determination of *Bulbus fritillariae cirrhosae* in Pharmacopoeia (State Pharmacopoeia Committee, 2015a), the ethanol extraction yields of FP, SP-I, and SP-II were determined by the hot dipping method. The dilute ethanol solution was prepared by diluting ethanol (529 ml) with water to 1,000 ml. BFU powder (2 g) was macerated with 50 ml dilute ethanol solution for 1 hr. The solution was heated and then kept slightly boiling for 1 hr. The total weight of flask, powder, and solvent was weighed before heating and the lost weight was restored. And the solution was filtered. The filtrate (25 ml) was placed in a dry evaporating dish, dried on a water bath. Then, the evaporating dish was dried at 105°C for 3 hr, cooled in a desiccator for 30 min, and weighed quickly and accurately. The ethanol extraction yield was calculated based on the increased weight of the evaporating dish after drying.

2.9 | Determination of total alkaloid content

The total alkaloid contents of FP, SP-I, and SP-II were measured by the content determination method for *Bulbus fritillariae cirrhosae* in Pharmacopoeia (State Pharmacopoeia Committee, 2015a).

2.10 | Determination of major alkaloids

2.10.1 | Sample preparation

Individual BFU powder (2 g) was prealkalized with 4 ml ammonium hydroxide for 1 hr, and mixed with 40 ml solution of trichloromethane–methanol (4:1, V/V). The mixtures were refluxed in 80°C water bath for 2 hr, the lost weight was restored, and the mixtures were filtrated. The filtrate (10 ml) was transferred to an evaporating dish and evaporated to dryness. The obtained residues were resolved with 2 ml methanol, and the resultant extracts were directly subjected to analysis.

2.10.2 | Chromatographic conditions

The samples were analyzed by Dionex U3000 HPLC system (Thermo Fisher), equipped with a pump and a CORONA Ultra Detector. An Eclipse XDB C18 column (150 mm × 4.6 mm I.D., 5 μm, Agilent) was utilized at a column temperature of 30°C. The mobile phase consisted of acetonitrile–methanol–water (65:10:25, v/v) containing 0.08% triethylamine with a flow rate of 1.0 ml/min. The evaporation temperature for detector was set at 30°C. Nitrogen was used as the carrier gas at a flow rate of 0.2 ml/min with the pressure of a nebulizing gas of 0.4 MPa. An aliquot (20 μl) of sample was injected.

2.11 | Fourier transform infrared spectroscopy (FTIR)

The FTIR spectra of FP, SP-I, and SP-II were collected via a Nicolet model 8700 spectrometer (Nicolet Instrument Corporation) in the wavenumber range of 400–4,000 cm^{-1} with a spectral resolution of 4 cm^{-1}. Samples were diluted with KBr mixing powder and pressed into self-supporting disks.

2.12 | X-ray diffraction (XRD)

In this study, X-ray diffraction analysis was employed to detect the crystallinity and was conducted using an XRD-6000 diffractometer (Shimadzu) in Bragg–Brentano geometry. The powder was placed in a glass sample holder. Subsequently, Cu Kα radiation was generated at 30 mA and 40 kV. Samples were scanned from 5° to 80° with a step size of 0.02°.

2.13 | Statistical analyses

Results were reported in conjunction with the standard deviation (*SD*). The differences in the mean were calculated using Duncan's multiple range tests with a 95% confidence limit ($p < .05$) and SPSS statics 22.0 software.

3 | RESULTS

3.1 | Particle size distribution and morphology

Table 1 and Figure 1 show the particle size distributions of BFU powders. After proper grinding, SP-I exhibited smaller particle size and smaller span value when compared to those of FP. Figure 1 also shows that the particles of FP were mainly distributed in the ranges of 0–80 μm and 80–600 μm and the particles of SP-I exhibited a concentrated distribution in the range of 0–70 μm. This indicates that significant particle size reduction in SP-I mainly resulted from the breakage

of large particles and the formation of smaller particles, which was similar to the particle size reduction of microcrystalline cellulose via grinding (Zheng, Fu, Li, & Wu, 2018). After intense grinding, SP-II exhibited smaller D_{90} and span value, but bigger D_{10} and D_{50} than FP. Additionally, the particles of SP-II were mainly distributed in the range of 0–200 μm. This suggests that the breakage of large particles and the agglomeration of individual particles existed simultaneously for SP-II, which was also similar to the breakage and agglomerative phenomena induced by prolonging grinding (Guzzo, Barros, & Tino, 2019; Zheng et al., 2018). Therefore, proper grinding significantly reduced the size of BFU powder and improved the particle size distribution.

The SEM images of different BFU powders are shown in Figure 2. For FP, particles with different sizes simultaneously existed with various particle shapes and a smooth particle surface. Various particle shapes were formed since the particles were squeezed during the growth process (Wang, 2006). For SP-I, particle sizes were similar, particle shapes were irregular, particle surfaces were rough, and the particle edges were broken, indicating that the main effect of grinding was the breaking of BFU particles (Zheng et al., 2018). For SP-II, broken particles and agglomeration of broken particles were observed. The SEM results were highly consistent with the particle size distribution results. The manufacturing of superfine powders was influenced by two counteracting processes: particle breakage and interparticle interaction (Austin & Bagga, 1981; Guzzo, Tino, & Santos, 2015). Particle breakage was considered to increase the specific surface area of the grinding product, and interparticle interactions governed by interfacial and surface properties were considered to reduce the specific surface area of grinding product (Guzzo et al., 2015). During grinding process, SP-I and SP-II underwent a morphological transformation under the effect of particle breakage and interparticle interaction (Fig. S1).

In particular, the agglomeration of superfine grinding particles was the typical behavior of powder system during grinding process (Opoczky, 1977). Huang, Lu, Li, and Tong (2007) reported that the formation of agglomeration in cassava starch by prolonging milling time was due to van der Waals force and electrostatic force. Zheng et al. (2018) also reported that the occurrence of agglomeration in microcrystalline cellulose by prolonging milling time was probably due to the high specific area and strong hydrogen bonds formed between the particles. With respect to the SP-II, the agglomeration of broken particles was due to the mechanical force and interparticle interactions. The increases in the size and the width of the size distribution of SP-II than SP-I should be caused by agglomerations (Guzzo et al., 2019; Sundum, Szécsényi, & Kaewtatip, 2018). Therefore, intense grinding of SP-II was unfavorable in terms of the particle size control of superfine BFU powder.

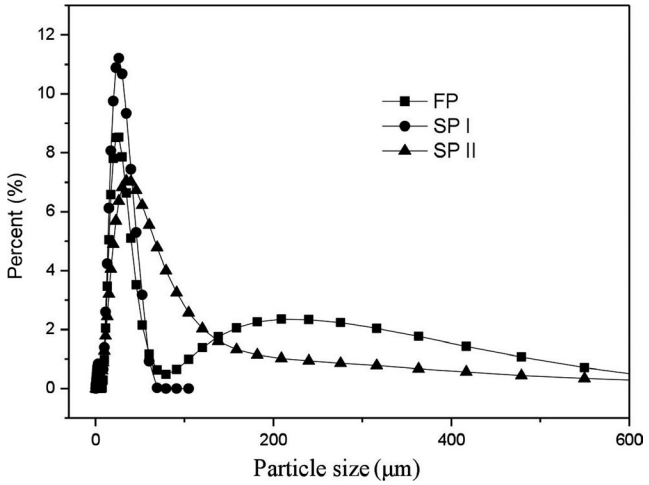

FIGURE 1 Particle size distributions of BFU powders. Particle size distributions of BFU powders shows particle size distribution curves of FP, SP-I, and SP-II. ■ represents FP (fine powder), ● represents SP-I (superfine powder I), and ▲ represents SP-II (superfine powder II)

3.2 | Physical properties of the BFU powder

The angle of repose reflects the change in the flowability of the powder (Ileleji & Zhou, 2008). As shown in Table 2, decreases in the particle size significantly increased the angle of repose of BFU powder, and this indicated that superfine powder exhibited decreased flowability. The result was in agreement with that stated in the reports (Huang, Dou, Li, & Wang, 2017; Zhao et al., 2014). According to Carr classification of flowability of powder based on repose angle (Al-Hashemi & Al-Amoudi, 2018; Riley & Hausner, 1970), SP-I was cohesive, and SP-II was fair to passable flow. Generally, angle of repose is related to

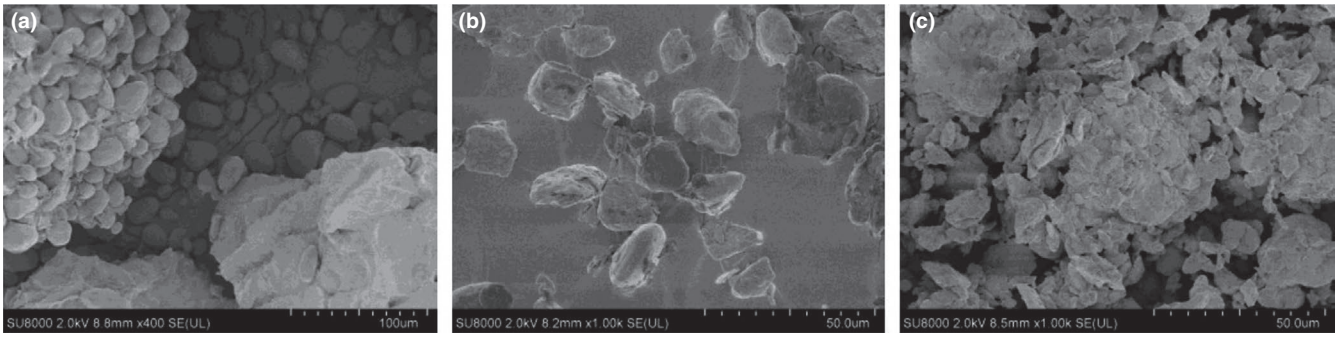

FIGURE 2 SEM images of (a) FP, (b) SP-I, and (c) SP-II. SEM images show the microstructures of BFU powders obtained by different methods. Image (a) corresponds to FP (fine powder, the particle size is 271.95 μm), image (b) corresponds to SP-I (superfine powder I, the particle size is 45.15 μm), and image (c) corresponds to SP-II (superfine powder II, the particle size is 154.02 μm)

TABLE 2 A angle of repose and bulk density of BFU powder (Mean ± *SD*, *n* = 5)

	Angle of repose (°)	Bulk density (g/ml)
FP	36.62 ± 2.79a	0.60 ± 0.00c
SP-I	49.50 ± 1.20c	0.49 ± 0.00b
SP-II	44.61 ± 3.44b	0.41 ± 0.00a

Note: Different lowercase letters in the same column indicate significant differences among the different treatments at the 0.05 level.

the interparticle force, interaction force, and the gravity force (Raei, Asadi, Moussavi, & Ghadiri, 2015; Wang et al., 2010). When particles were small, the interparticle forces became dominant (Wang et al., 2010; Yang, Liu, Yang, & Cao, 2009). Lumay et al. (2012) also reported that the cohesion between the particles could affect the angle of repose when the particle sizes of flours were lower than 50 μm. Therefore, the decreased flowability was potential because the decrease in particle size increased the particle surface area per unit mass, providing a greater surface area for cohesive force to interact (Jan, Karde, Ghoroi, & Saxena, 2018). Superfine grinding treatment adversely affected the flowability of the BFU powder, which would result in blockage, unstable discharge, and subsequent stoppage of the equipment and processes (Garg, Mallick, Trinanes, & Berry, 2018).

The bulk density is often used to characterize powder flow behavior, significantly affecting material handling and storage aspects (Vasilenko, Koynov, Glasser, & Muzzio, 2013; Zhao et al., 2013, 2010). The bulk density depends on multiple factors, such as particle size and shape, environmental conditions, and consolidating stress (Vasilenko et al., 2013). As shown in Table 2, the bulk density of FP (0.60 g/ml) with a D_{90} size of 271.95 μm exceeded that of SP-I and SP-II, and this was not in agreement with the results stated in the reports (Wu, Zhang, Wang, Mothibe, & Chen, 2012; Zhao et al., 2014). The low bulk density should be due to unusually large voidage between the particles (Shenoy et al., 2015; Zhao, Zhu, Zhang, & Tang, 2015). Pai and Okos (2013) demonstrated that for an assembly of small and large particles, as the proportion of smaller particles exceeded a certain value, bulk density decreased because of increased voidage between smaller particles. Mohammadi and Harnby (1997) and Liu, Lu, Poletto, Guo, and Gong (2017) also reported that when the particle size was small, interparticle forces were comparable with the particle weight and prevented particles from forming compact structures, which resulted in low-density values and cohesive bulk powders. Additionally, the bulk density of SP-II (0.41 g/ml) with a D_{90} size of 154.02 μm was lower than that of SP-I. Furthermore, the BFU powder with lower bulk density will be adverse to the robustness of the process and the quality of final product, such as packing behavior, filling behavior in preparing tablets or capsule products (Vasilenko et al., 2013; Zhao et al., 2010).

The moisture absorption of material refers to its ability to absorb water under certain conditions of temperature and humidity, which can be used as a reference to select suitable pharmaceutical packaging and storage conditions (State Pharmacopoeia Committee, 2015b). A relatively large amount of moisture absorbed in powder significantly impacts the long-term stability and performance of powder (Yu, Romeo, Cavallaro, & Chan, 2018). As shown in Table 3, there were no significant differences among BFU powders, thereby indicating that superfine grinding did not significantly influence the moisture absorption property of BFU powder. This was potentially related to the formation of a dense film on the BFU powder surface after certain moisture absorption, which blocked the diffusion path of moisture (Joshi & Petereit, 2013; Zhao et al., 2014). Additionally, the percentages of moisture absorption of BFU powders were more than 2%, but less than 15%, thereby indicating that BFU powder exhibited hygroscopicity (State Pharmacopoeia Committee, 2015b).

Swelling capacity is an important parameter that reflects the hydration ability. As shown in Table 3, the swelling capacities of SP-I and SP-II increased by 0.82 ml/g and 5.90 ml/g, respectively, when compared with the swelling capacity of FP (1.93 ml/g). Generally, it is difficult for water to enter the starch granules through the pores (Zhang et al., 2019). Given that increased surface area, polar groups, and other water-binding sites were exposed to the surrounding water medium, the increased swelling capacities of SP-I and SP-II potentially related to the decreases in the size of BFU particles (Du, Zhu, & Xu, 2014). The stronger swelling capacity of SP-II than that of SP-I should be due to the fact that the active sites in starch granules increased as a result of the structure destruction of starch under intense grinding treatment (Hofmann et al., 2018; Pineda, Ojeda, Romero, Balu, & Luque, 2018). Previously, a similar pattern was observed for the greatly improved swelling capacity of acetylated starch by grinding (Zhang et al., 2019). Thus, superfine grinding treatment enhanced the swelling capacity of the BFU powder.

3.3 | Ethanol extraction yield and alkaloid content

Plant extracts contain compounds that exhibit synergistic pharmacological effects (Yang et al., 2014), and thus, plant extraction yield is typically used as an index to measure the quality of a traditional

TABLE 3 Moisture adsorption, swelling capacity, ethanol extraction yield, and total alkaloid content of BFU powder (Mean ± *SD*, *n* = 3)

	Moisture adsorption (%)	Swelling capacity (ml/g)	Ethanol extraction yield (%)	Total alkaloid content (%)
FP	9.41 ± 2.16a	1.93 ± 0.15a	4.39 ± 0.25a	0.009 ± 0.001a
SP-I	8.73 ± 0.92a	2.75 ± 0.30b	5.67 ± 0.26b	0.015 ± 0.001c
SP-II	8.67 ± 2.47a	7.83 ± 0.24c	7.78 ± 0.90c	0.011 ± 0.001b

Note: Different lowercase letters in the same column indicate significant differences among the different treatments at the 0.05 level.

TABLE 4 Contents of isosteroidal alkaloids in BFU powders (Mean ± *SD*, *n* = 3)

	Peimissine (μg/g)	Imperialine (μg/g)	Verticine (μg/g)	Verticinone (μg/g)
FP	65.12 ± 2.67b	14.49 ± 0.54c	13.47 ± 1.83a	2.65 ± 0.20a
SP-I	72.35 ± 3.70a	23.32 ± 0.92a	13.40 ± 2.57a	2.57 ± 0.19a
SP-II	59.23 ± 2.96b	20.29 ± 0.73b	13.83 ± 1.93a	2.94 ± 0.37a

Note: Different lowercase letters in the same column indicate significant differences among the different treatments at the 0.05 level.

Chinese herb. The ethanol extraction yields obtained from BFU powders are shown in Table 3. When compared to FP, the ethanol extraction yield of SP-I increased by 29.2%. It is commonly accepted that smaller particles with higher specific surface enhanced the diffusion of chemical components (Huang, Li, & Wang, 2018). Similar results were observed for the extraction of superfine black tea powder (Xiao et al., 2017). Additionally, the ethanol extraction yield of SP-II also exceeded that of SP-I. As expected, superfine grinding significantly improved the ethanol extraction yield.

The total alkaloid contents of BFU powders are determined and shown in Table 3. Decreases in the D_{90} size of BFU powder from 271.95 μm to 45.15 μm significantly increased the total alkaloid content from 0.009% to 0.015%. When compared to FP, the total alkaloid content of SP-I increased by 66.7%. Chen et al. (2014) also reported that the verticine dissolution rate of *Fritillaria thunbergii* Miq. superfine powder (D_{50} = 36.46 μm) was 59.5% higher than that of common powder (D_{50} = 158.65 μm). The increasing tendency of the total alkaloid content was observed with reductions in the particle size (Xiao et al., 2017). Research on the effect of superfine grinding on the properties of red grape pomace powders indicated that total polyphenolic content was improved by superfine grinding from 450.13 mg/100 g to 757.36 mg/100 g (Zhao et al., 2015). Zhao et al. (2009) also reported that the protein solubility of ginger powder increased with decreasing particle size from 300 to 8.34 μm. Xiao et al. (2017) attributed the higher caffeine yield of superfine black tea powder to the smaller particles with higher particle surface area. Li, Li, Liu, and Yin (2007) reported that the breakage of cell wall by superfine grinding also could greatly reduce the mass transfer resistance and enhance the diffusion of active ingredients. Therefore, the significant increase in alkaloids content of SP-I can be integrated from the increase in particle surface area and the breakdown of the cell walls, indicating that the particle size was a key parameter associated with the release of active components (Astill, Birch, Dacombe, Humphrey, & Martin, 2001).

Furthermore, the contents of 4 alkaloids in different BFU powders were determined and are shown in Table 4. For the type A isosteroidal alkaloids, peimissine, verticine, and verticinone were found in almost all Beimu herbs; for the type B isosteroidal alkaloid, imperialine was detected in Chuan-Beimu, Ping-Beimu, Yi-Beimu (Li, Li, Lin, Chan, & Ho, 2000). As shown in Table 4, there were no significant differences in the contents of verticine and verticinone among BFU powders. When compared to FP, the peimissine and imperialine contents of SP-I increased significantly. When compared to FP, the peimissine content of SP-II did not change significantly, and the imperialine content of SP-II increased significantly. The increases in the peimissine and imperialine contents should be also attributed to the increase in particle surface area and the breakdown of the cell walls (Astill et al., 2001; Li et al., 2007). In addition, it can be seen from Table 4 that the contents of peimissine and imperialine were higher among 4 alkaloids in BFU powders. Zhou et al. (2008) reported that the content of peimissine was 68.92 μg/g, the contents of imperialine and verticine in *F. unibracteata* were at trace level, and the content of verticinone could not be detected. Zhou, Guo, Shen, Chen, and Qin (2014) found that the contents of peimissine, verticine, and verticinone in *F. unibracteata* were 21.5–24.1 μg/g, 65.8–81.4 μg/g, and at undetected level, separately. Wu et al. (2018) reported that the contents of imperialine and verticine & verticinone in *F. unibracteata* were 39.04 μg/g and 301.11 μg/g. These results confirmed the existence of peimissine and imperialine in BFU powders.

Therefore, the application of superfine grinding technology in BFU powder increased the extraction efficiency and improved the functional ingredient contents.

3.4 | FTIR analysis

FTIR spectra of BFU powders are obtained and shown in Figure 3. For FP, the peaks at 3,440 and 2,900 cm^{-1} were due to the OH bonds and CH_2 deformation, respectively (Dankarab, Haddaraha, Omara, Pujolàb, & Sepulcreb, 2018; Kacuráková & Mathlouthi, 1996). The peaks at 1,650 cm^{-1} were attributed to the absorbed H_2O bending vibration (Kizil, Irudayaraj, & Seetharaman, 2002). The peaks at 1,163 cm^{-1} and 1,080 cm^{-1} were caused by C-O stretching and anhydroglucose ring O–C stretching (Fang, Fowler, Tomkinson, & Hill, 2002; Warren, Gidley, & Flanagan, 2016). The bands at 1,047 cm^{-1} and 1,016 cm^{-1} were characteristic of the ordered and amorphous structure of starch (Liu, Ma, Yu, Shi, & Xue, 2011; Lopez-Rubio, Flanagan, Shrestha, Gidley, & Gilbert, 2008).

As shown in Figure 3, SP-I and SP-II did not show any obvious new peaks. This indicates that no new functional groups were produced after superfine grinding. However, the intensities of peaks at the range of 1,000–1,650 cm^{-1} decreased after proper grinding, which should be mainly resulted from the particle size reduction (Tan et al., 2015; Zhao et al., 2013). After intense grinding, the intensities of peaks at 3,440 and 1,016 cm^{-1} increased, the peak at 1,047 cm^{-1} almost disappeared, and the intensity of peak at 985 cm^{-1} decreased. Liu et al. (2011) reported that the intensities of bands at 3,382 cm^{-1} in the treated maize starch spectra increased with the increase in grinding strength, which might be due to the transformation of hydrogen bond vibration mode caused by grinding treatment. The intensity change in bands at 985 cm^{-1}, 1,016 cm^{-1}, and 1,047 cm^{-1} should be due to the destroyed crystalline structure of starch in SP-II (Ambigaipalan et al., 2011; Blaszczak, Valverde, & Fornal, 2005;

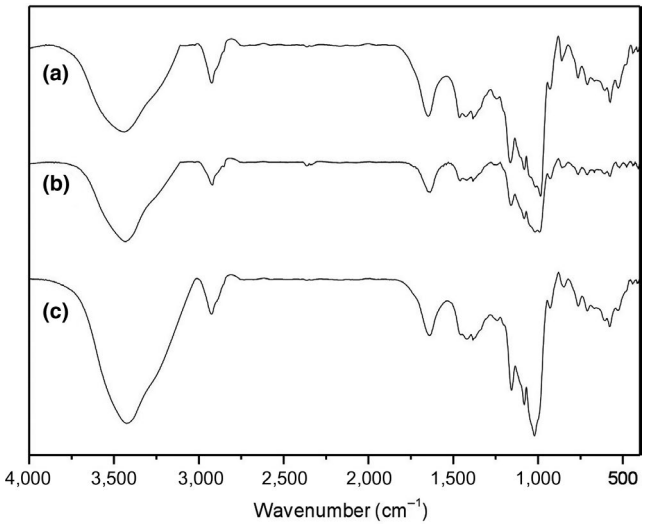

FIGURE 3 FTIR spectra of BFU powders: (a) FP; (b) SP-I; (c) SP-II. FTIR spectra show the chemical composition information of BFU powders obtained by different methods. Line (a) corresponds to FP (fine powder, the particle size is 271.95 μm), line (b) corresponds to SP-I (superfine powder I, the particle size is 45.15 μm), and line (c) corresponds to SP-II (superfine powder II, the particle size is 154.02 μm)

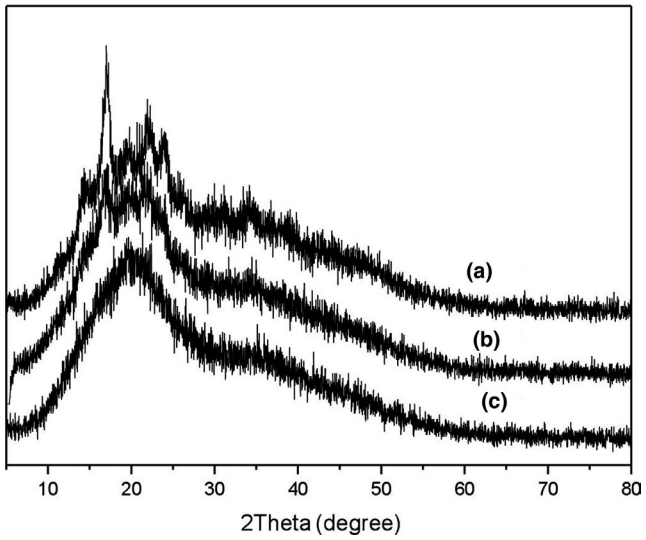

FIGURE 4 XRD patterns of BFU powders: (a) FP; (b) SP-I; (c) SP-II. XRD patterns show the crystalline structure information of BFU powders obtained by different methods. Line (a) corresponds to FP (fine powder, the particle size is 271.95 μm), line (b) corresponds to SP-I (superfine powder I, the particle size is 45.15 μm), and line (c) corresponds to SP-II (superfine powder II, the particle size is 154.02 μm)

Huang et al., 2007; Xie, Liu, & Cui, 2006). The crystalline structure of starch would be further demonstrated in X-ray diffraction section.

3.5 | XRD analysis

A starch granule exhibits a semicrystalline structure that comprises of crystalline and amorphous regions (Niu, Zhang, Jia, & Zhao, 2017). The ordered three-dimensional structure of the amylopectin segment is associated with the crystallinity of starch granules (Bayer, Cagiao, & Calleja, 2006; Zobel, 1988).

To understand the changes in crystalline structure, the XRD curves of different BFU powders obtained after different processing treatments were obtained. With respect to the FP, an intense peak was observed at approximately 17° and a few peaks were observed at 15°, 20°, 22°, and 24° as well. The observed peaks of FP also indicate that the crystal type of BFU corresponded to type B, and this was consistent with Wang et al. (2007) and Martínez et al. (2019) results. After proper grinding, a few weak peaks were observed at 17°, 20°, and 22° for SP-I. Furthermore, after intense grinding, SP-II exhibited peaks at 20° and 22°. The XRD results indicate that the crystalline peak intensities were gradually reduced with enhancements in the grinding strength, which reflected the decrease in crystallinity (Martínez-Bustos, López-Soto, San Martín-Martínez, Zazueta-Morales, & Velez-Medina, 2007). This observation was in accordance with the report about maize starch (Liu et al., 2011).

Crystallinity in starch is determined by the following: (a) crystal size, (b) percentage of crystalline regions, (c) orientation of the double helices within the crystalline domains, and (d) extent of interaction between double helices (Hoover & Ratnayake, 2002). According to Hebeish, El-Rafie, El-Sheikh, and El-Naggar (2014), the reduction in starch crystallite size arising from the reduction in particle size during grinding process could result in a decrease and disappearance of diffraction peaks. This reason is that small crystallites may not produce enough detectable reflection intensities, especially for carbon element (Augustine et al., 2019). Lv et al. (2019) and Tan et al. (2015) also reported that the destruction of the starch crystalline structure could result in a less intense or partly disappeared diffraction peak. Additionally, Martínez-Bustos et al. (2007) attributed a partial loss of starch crystallinity to a temperature increase, resulted from mechanical energy conduction or dissipation during grinding process. Therefore, the decrease in intensity and the disappearance of diffraction peaks were mainly attributed to the reduction in crystallite size and the destruction of the crystalline structure.

In general, for all BFU powders, the peak centered at 20° is observed (Figure 4). Normally, amylose–lipid complexes were indicated by a 20° peak, but the complexes were also characterized by two other peaks at 7° and 13° (Godet, Bizot, & Buléon, 1995; Lopez-Rubio, Flanagan, Gilbert, & Gidley, 2008). Lopez-Rubio, Flanagan, Gilbert, et al. (2008) assumed that a 20° peak of wheat and rice was mainly due to ordered single amylose helices. Varatharajan et al. (2011) reported that the peak at 20° was due to single left-handed linear starch chains. From these results, it could be concluded that the structure of starch chains was not destroyed seriously during grinding process.

4 | DISCUSSION

The grinding process of starch granules was divided into three stages: stress, aggregation, and agglomeration (Zhang et al., 2018).

At agglomeration stage, some fragments adhered to the broke starch granule and some fragments agglomerated together. Guzzo et al. (2019) also reported that a strong competition between breakage and agglomeration mechanisms occurred in dry grinding process. The change from breakage to agglomeration can be suggested by large-size agglomerates. In our research, SP-I exhibited rough particles with broken edges and similar sizes, and SP-II exhibited agglomeration of broken particles. This indicates that the breakage was dominant in SP-I, and the agglomeration was dominant in SP-II (Zheng et al., 2018). Thus, grinding treatment had a marked mechanochemical effect on BFU powders.

Previous studies reported that the particle size might have a positive or negative correlation effect on powder physicochemical properties; for instance, the particle size might have a negative correlation effect ($p < .05$) on the density characteristics (He et al., 2017; Zhao et al., 2015). In our study, the size was smaller for BFU powders, greater for the angle of repose (from 36.62 to 49.50°) and total alkaloid content (from 0.009% to 0.015%). However, the bulk density, swelling capacity, and ethanol extraction yield in our study were not consistent with the findings due to the performance of SP-II. This may be potentially related to the occurrence of agglomeration and structure change induced by intense superfine grinding (Guzzo et al., 2019; Huang et al., 2007). Opoczky (1977) also reported that agglomeration had a negative effect on certain properties of the grinding product. Guzzo et al. (2019) reported that the ability of grinding product to hydrate, reactivity, and solubility could be negatively affected because of agglomeration and structural changes induced by high-energy milling. Hu, Chen, and Ni (2012) and Zhao et al. (2015) indicated that the higher temperature induced by intense grinding would affect the stability of active content in superfine powders. Thus, even though particle size may significantly affect the properties of BFU powder, other phenomena (agglomeration, structure change, etc.) induced by intense grinding also have a significant effect on certain properties.

Decreases in the D_{90} size of BFU powder from 271.95 to 45.15 μm significantly increased the ethanol extraction yield, total alkaloid content, and the contents of the peimissine and imperialine. FTIR results indicate that no new functional groups produced after superfine grinding. XRD results indicate the decreased crystallinity after superfine grinding. It was reported that superfine grinding markedly increased the extraction of active ingredients, leading to improved bioavailability and bioactivity in vivo or in vitro (Hu et al., 2012; Tao et al., 2014; Xiao et al., 2017). Therefore, the application of superfine grinding in BFU powders exhibits positive significance in terms of increasing the bioavailability of BFU and saving material resources.

5 | CONCLUSIONS

In this study, three bulbs of *F. unibracteata* Hsiao et K.C. Hsia (BFU) powders in different sizes were produced via superfine and conventional grinding methods. Particle size and grinding process played an important role in the properties of BFU powders. Specifically, SP-I exhibited the smallest particle size and the narrowest particle size distribution. Additionally, SP-I exhibited significantly high total alkaloid content and ethanol extraction yield. This is due to the increase in particle surface area and the breakdown of the cell walls. Although particle size may significantly affect the properties of BFU powder, other phenomena (agglomeration, structure change, etc.) induced by intense grinding also have a significant effect on certain properties. Superfine grinding technology improved utilization efficiency in BFU consumption and displayed the potential to expand the application of BFU powder in the health food and Chinese herb industry.

ACKNOWLEDGMENTS

This work was supported by the Natural Science Foundation of Qinghai Province for Young Scholars (No. 2016-ZJ-958Q); the Development Project of Qinghai Provincial Key Laboratory (No. 2017-ZJ-Y10); the Capacity Building Project of Engineering Research Center of Qinghai Province (No. 2017-GX-G03).

CONFLICT OF INTEREST

The authors declare that they do not have any conflict of interest.

ETHICAL APPROVAL

This study does not involve any human or animal testing.

ORCID

Shi-zhen Ma https://orcid.org/0000-0002-8547-9609

REFERENCES

Al-Hashemi, H. M. B., & Al-Amoudi, O. S. B. (2018). A review on the angle of repose of granular materials. *Powder Technology*, *330*, 397–417. https://doi.org/10.1016/j.powtec.2018.02.003

Ambigaipalan, P., Hoover, R., Donner, E., Liu, Q., Jaiswal, S., Chibbar, R., … Seetharaman, K. (2011). Structure of faba bean, black bean and pinto bean starches at different levels of granule organization and their physicochemical properties. *Food Research International*, *44*, 2962–2974. https://doi.org/10.1016/j.foodres.2011.07.006

Astill, C., Birch, M. R., Dacombe, C., Humphrey, P. G., & Martin, P. T. (2001). Factors affecting the caffeine and polyphenol contents of black and green tea infusions. *Journal of Agricultural and Food Chemistry*, *49*, 5340–5347. https://doi.org/10.1021/jf010759+

Augustine, A., Junin, R., Gbadamosi, A. O., Abbas, A., Azli, N. B., & Oseh, J. (2019). Influence of nanoprecipitation on crystalline starch nanoparticle formed by ultrasonic assisted weak-acid hydrolysis of cassava starch and the rheology of their solutions. *Chemical Engineering and Processing: Process Intensification*, *142*, 107556.

Austin, L. G., & Bagga, P. (1981). An analysis of fine dry grinding in ball mills. *Powder Technology*, *28*, 83–90. https://doi.org/10.1016/0032-5910(81)87014-3

Bayer, R. K., Cagiao, M. E., & Calleja, F. J. B. (2006). Structure development in amorphous starch as revealed by X-ray scattering: Influence of the network structure and water content.

Journal of Applied Polymer Science, *99*(4), 1880–1886. https://doi.org/10.1002/app.22655

Blaszczak, W., Valverde, S., & Fornal, J. (2005). Effect of high pressure on the structure of potato starch. *Carbohydrate Polymers*, *59*(3), 377–383. https://doi.org/10.1016/j.carbpol.2004.10.008

Chen, B., Ai, G., & Huang, Z. (2014). Influence of partical diameter on dissolution rate in vitro and pharmacodynamics of *Fritillaria Thunbergii* Miq. *Chinese Archives of Traditional Chinese Medicine*, *32*, 1999–2001.

Dankarab, I., Haddaraha, A., Omara, F. E. L., Pujolàb, M., & Sepulcreb, F. (2018). Characterization of food additive-potato starch complexes by FTIR and X-ray diffraction. *Food Chemistry*, *260*, 7–12. https://doi.org/10.1016/j.foodchem.2018.03.138

Du, B., Zhu, F., & Xu, B. (2014). Physicochemical and antioxidant properties of dietary fibers from Qingke (hull-less barley) flour as affected by ultrafine grinding. *Bioactive Carbohydrates and Dietary Fibre*, *4*, 170–175. https://doi.org/10.1016/j.bcdf.2014.09.003

Fang, J. M., Fowler, P. A., Tomkinson, J., & Hill, C. A. S. (2002). The preparation and characterisation of a series of chemically modified potato starches. *Carbohydrate Polymers*, *47*, 245–252. https://doi.org/10.1016/S0144-8617(01)00187-4

Gao, W. Y., Fan, L., & Paek, K. Y. (1999). Ultrastructure of amyloplasts and intercellular transport of old and new scales in *Fritillaria ussuriensis*. *Journal of Plant Biology*, *42*, 117–123. https://doi.org/10.1007/BF03031019

Garg, V., Mallick, S. S., Trinanes, P. G., & Berry, R. J. (2018). An investigation into the flowability of fine powders used in pharmaceutical industries. *Powder Technology*, *336*, 375–382. https://doi.org/10.1016/j.powtec.2018.06.014

Godet, M. C., Bizot, H., & Buléon, A. (1995). Crystallization of amylose-fatty acid complexes prepared with different amylose chain lengths. *Carbohydrate Polymers*, *27*(1), 47–52.

Guzzo, P. L., Barros, F. B. M., & Tino, A. A. A. (2019). Effect of prolonged dry grinding on size distribution, crystal structure and thermal decomposition of ultrafine particles of dolostone. *Powder Technology*, *342*, 141–148. https://doi.org/10.1016/j.powtec.2018.09.064

Guzzo, P. L., Tino, A. A. A., & Santos, J. B. (2015). The onset of particle agglomeration during the dry ultrafine grinding of limestone in a planetary ball mill. *Powder Technology*, *284*, 122–129. https://doi.org/10.1016/j.powtec.2015.06.050

Hao, D. C., Gu, X. J., Xiao, P. G., & Peng, Y. (2013). Phytochemical and biological research of *Fritillaria* medicine resources. *Chinese Journal of Natural Medicines*, *11*, 330–344. https://doi.org/10.1016/S1875-5364(13)60050-3

He, S., Li, J., He, Q., Jian, H., Zhang, Y., Wang, J., & Sun, H. (2017). Physicochemical and antioxidant properties of hard white winter wheat (*Triticum aestivm* L.) bran superfine powder produced by eccentric vibratory milling. *Powder Technology*, *325*, 126–133. https://doi.org/10.1016/j.powtec.2017.10.054

Hebeish, A., El-Rafie, M. H., El-Sheikh, M. A., & El-Naggar, M. E. (2014). Ultra-fine characteristics of starch nanoparticles prepared using native starch with and without surfactant. *Journal of Inorganic and Organometallic Polymers and Materials*, *24*, 515–524. https://doi.org/10.1007/s10904-013-0004-x

Hofmann, F., Harder, R. J., Liu, W., Liu, Y., Robinson, I. K., & Zayachuk, Y. (2018). Glancing-incidence focussed ion beam milling: a coherent X-ray diffraction study of 3D nano-scale lattice strains and crystal defects. *Acta Materialia*, *154*, 113–123.

Hoover, R., & Ratnayake, W. S. (2002). Starch characteristics of black bean, chick pea, lentil, navy bean and pinto bean cultivars grown in Canada. *Food Chemistry*, *78*, 489–498. https://doi.org/10.1016/S0308-8146(02)00163-2

Hu, J. H., Chen, Y. Q., & Ni, D. J. (2012). Effect of superfine grinding on quality and antioxidant property of fine green tea powders. *LWT - Food Science and Technology*, *45*, 8–12. https://doi.org/10.1016/j.lwt.2011.08.002

Huang, X., Dou, J. Y., Li, D., & Wang, L. J. (2017). Effects of superfine grinding on properties of sugar beet pulp powders. *LWT-Food Science and Technology*, *87*, 203–209. https://doi.org/10.1016/j.lwt.2017.08.067

Huang, X., Li, D., & Wang, L. J. (2018). Effect of particle size of sugar beet pulp on the extraction and property of pectin. *Journal of Food Engineering*, *218*, 44–49. https://doi.org/10.1016/j.jfoodeng.2017.09.001

Huang, Z. Q., Lu, J. P., Li, X. H., & Tong, Z. F. (2007). Effect of mechanical activation on physico-chemical properties and structure of cassava starch. *Carbohydrate Polymers*, *68*(1), 128–135. https://doi.org/10.1016/j.carbpol.2006.07.017

Ileleji, K. E., & Zhou, B. (2008). The angle of repose of bulk corn stover particles. *Powder Technology*, *187*, 110–118. https://doi.org/10.1016/j.powtec.2008.01.029

Jan, S., Karde, V., Ghoroi, C., & Saxena, D. C. (2018). Effect of particle and surface properties on flowability of rice flours. *Food Bioscience*, *23*, 38–44. https://doi.org/10.1016/j.fbio.2018.03.001

Joshi, S., & Petereit, H. U. (2013). Film coatings for taste masking and moisture protection. *International Journal of Pharmaceutics*, *457*, 395–406. https://doi.org/10.1016/j.ijpharm.2013.10.021

Kacuráková, M., & Mathlouthi, M. (1996). FTIR and laser-Raman spectra of oligosaccharides in water: Characterization of the glycosidic bond. *Carbohydrate Research*, *284*, 145–157. https://doi.org/10.1016/0008-6215(95)00412-2

Kizil, R., Irudayaraj, J., & Seetharaman, K. (2002). Characterization of irradiated starches by using FT-Raman and FTIR spectroscopy. *Journal of Agricultural and Food Chemistry*, *50*, 3912–3918. https://doi.org/10.1021/jf011652p

Li, C. H., Li, W., Liu, X. X., & Yin, D. H. (2007). Prior cell wall breakage and extraction of fine ginger oil with supercritical CO_2. *Industrial and Engineering Chemistry Research*, *26*(9), 1294–1299 (in Chinese).

Li, S. L., Li, P., Lin, G., Chan, S. W., & Ho, Y. P. (2000). Simultaneous determination of seven major isosteroidal alkaloids in bulbs of *Fritillaria* by gas chromatography. *Journal of Chromatography A*, *873*, 221–228. https://doi.org/10.1016/S0021-9673(00)00049-2

Li, S., Liu, J., Gong, X., Yang, X., Zhu, Y., & Cheng, Z. (2013). Characterizing the major morphological traits and chemical compositions in the bulbs of widely cultivated *Fritillaria* species in China. *Biochemical Systematic and Ecology*, *46*, 130–136. https://doi.org/10.1016/j.bse.2012.09.014

Li, X., Dai, Y., & Chen, S. (2009). Growth and physiological characteristics of *Fritillaria cirrhosa* in response to high irradiance and shade in age-related growth phases. *Environmental and Experimental Botany*, *67*, 77–83. https://doi.org/10.1016/j.envexpbot.2009.07.005

Liu, T. Y., Ma, Y., Yu, S. F., Shi, J., & Xue, S. (2011). The effect of ball milling treatment on structure and porosity of maize starch granule. *Innovative Food Science and Emerging Technologies*, *12*, 586–593. https://doi.org/10.1016/j.ifset.2011.06.009

Liu, Y., Lu, H., Poletto, M., Guo, X., & Gong, X. (2017). Bulk flow properties of pulverized coal systems and the relationship between inter-particle forces and particle contacts. *Powder Technology*, *322*, 226–240.

Lopez-Rubio, A., Flanagan, B. M., Gilbert, E. P., & Gidley, M. J. (2008). A novel approach for calculating starch crystallinity and its correlation with double helix content: A combined XRD and NMR study. *Biopolymers*, *89*, 761–768. https://doi.org/10.1002/bip.21005

Lopez-Rubio, A., Flanagan, B. M., Shrestha, A. K., Gidley, M. J., & Gilbert, E. P. (2008). Molecular rearrangement of starch during in vitro digestion: Toward a better understanding of enzyme resistant starch formation in processed starches. *Biomacromolecules*, *9*, 1951–1958. https://doi.org/10.1021/bm800213h

Lumay, G., Boschini, F., Traina, K., Bontempi, S., Remy, J. C., Cloots, R., & Vandewalle, N. (2012). Measuring the flowing properties of powders and grains. *Powder Technology*, *224*, 19–27. https://doi.org/10.1016/j.powtec.2012.02.015

Lv, Y., Zhang, L., Li, M., He, X., Hao, L., & Dai, Y. (2019). Physicochemical properties and digestibility of potato starch treated by ball milling with tea polyphenols. *International Journal of Biological Macromolecules*, *129*, 207–213. https://doi.org/10.1016/j.ijbiomac.2019.02.028

Martínez, P., Peña, F., Bello-Pérez, L. A., Núñez-Santiago, C., Yee-Madeira, H., & Velezmoro, C. (2019). Physicochemical, functional and morphological characterization of starches isolated from three native potatoes of the Andean region. *Food Chemistry: X*, *2*, 100030.

Martínez-Bustos, F., López-Soto, M., San Martín-Martínez, E., Zazueta-Morales, J. J., & Velez-Medina, J. J. (2007). Effects of high energy milling on some functional properties of jicama starch (*Pachyrrhizus erosus* L. Urban) and cassava starch (*Manihot esculenta* Crantz). *Journal of Food Engineering*, *78*, 1212–1220. https://doi.org/10.1016/j.jfoodeng.2005.10.043

Mohammadi, M. S., & Harnby, N. (1997). Bulk density modelling as a means of typifying the microstructure and flow characteristics of cohesive powders. *Powder Technology*, *92*(1), 1–8. https://doi.org/10.1016/S0032-5910(96)03254-8

Niu, M., Zhang, B., Jia, C., & Zhao, S. (2017). Multi-scale structures and pasting characteristics of starch in whole-wheat flour treated by superfine grinding. *International Journal of Biological Macromolecules*, *104*, 837–845. https://doi.org/10.1016/j.ijbiomac.2017.06.125

Opoczky, L. (1977). Fine grinding and agglomeration of silicates. *Powder Technology*, *17*, 1–7. https://doi.org/10.1016/0032-5910(77)85037-7

Pai, D. A., & Okos, M. R. (2013). Predicting the density and tensile strength of viscoelastic soy powder compacts. *Journal of Food Engineering*, *116*, 184–194. https://doi.org/10.1016/j.jfoodeng.2012.10.043

Pineda, A., Ojeda, M., Romero, A. A., Balu, A. M., & Luque, R. (2018). Mechanochemical synthesis of supported cobalt oxide nanoparticles on mesoporous materials as versatile bifunctional catalysts. *Microporous & Mesoporous Materials*, *272*, 129–136.

Raei, B., Asadi, H., Moussavi, A., & Ghadiri, H. (2015). A study of initial motion of soil aggregates in comparison with sand particles of various sizes. *Catena*, *127*, 279–286. https://doi.org/10.1016/j.catena.2014.12.031

Riley, R. E., & Hausner, H. H. (1970). Effect of particle size distribution on the friction in a powder mass. *International Journal of Powder Metallurgy*, *6*, 17–22.

Shenoy, P., Viau, M., Tammel, K., Innings, F., Fitzpatrick, J., & Ahrne, L. (2015). Effect of powder densities, particle size and shape on mixture quality of binary food powder mixtures. *Powder Technology*, *272*, 165–172. https://doi.org/10.1016/j.powtec.2014.11.023

State Pharmacopoeia Committee (2015a). *Pharmacopoeia of People's Republic of China Part I* (10th ed.). Beijing: China: Medical Science Press.

State Pharmacopoeia Committee (2015b). *Pharmacopoeia of People's Republic of China Part IV* (10th ed.). Beijing: China: Medical Science Press.

Sundum, T., Szécsényi, K. M., & Kaewtatip, K. (2018). Preparation and characterization of thermoplastic starch composites with fly ash modified by planetary ball milling. *Carbohydrate Polymers*, *191*, 198–204. https://doi.org/10.1016/j.carbpol.2018.03.009

Tan, X., Zhang, B., Chen, L., Li, X., Li, L., & Xie, F. (2015). Effect of planetary ball-milling on multi-scale structures and pasting properties of waxy and high-amylose cornstarches. *Innovative Food Science and Emerging Technologies*, *30*, 198–207. https://doi.org/10.1016/j.ifset.2015.03.013

Tao, B., Ye, F., Li, H., Hu, Q., Xue, S., & Zhao, G. (2014). Phenolic profile and in vitro antioxidant capacity of insoluble dietary fiber powders from Citrus (*Citrus junos* Sieb. ex Tanaka) pomace as affected by ultrafine grinding. *Journal of Agricultural and Food Chemistry*, *62*, 7166–7173.

Varatharajan, V., Hoover, R., Li, J., Vasanthan, T., Nantanga, K. K. M., Seetharaman, K., … Chibbare, R. N. (2011). Impact of structural changes due to heat-moisture treatment at different temperatures on the susceptibility of normal and waxy potato starches towards hydrolysis by porcine pancreatic alpha amylase. *Food Research International*, *44*(9), 2594–2606. https://doi.org/10.1016/j.foodres.2011.04.050

Vasilenko, A., Koynov, S., Glasser, B. J., & Muzzio, F. J. (2013). Role of consolidation state in the measurement of bulk density and cohesion. *Powder Technology*, *239*, 366–373. https://doi.org/10.1016/j.powtec.2013.02.011

Wang, S. (2006). *Study on starch in starch-rich Chinese Fritillaria and Chinese Yam* (Doctoral dissertation), Tianjin University, Tianjin.

Wang, S., Yu, J., Gao, W., Pang, J., Yu, J., & Xiao, P. (2007). Comparison of starches separated from three different *F. cirrhosa*. *Journal of Food Engineering*, *80*, 417–422. https://doi.org/10.1016/j.jfoodeng.2006.01.087

Wang, W., Zhang, J., Yang, S., Zhang, H., Yang, H., & Yue, G. (2010). Experimental study on the angle of repose of pulverized coal. *Particuology*, *8*, 482–485. https://doi.org/10.1016/j.partic.2010.07.008

Warren, F. J., Gidley, M. J., & Flanagan, B. M. (2016). Infrared spectroscopy as a tool to characterise starch ordered structure-a joint FTIR-ATR, NMR, XRD and DSC study. *Carbohydrate Polymers*, *139*, 35–42. https://doi.org/10.1016/j.carbpol.2015.11.066

Wu, G. C., Zhang, M., Wang, Y. Q., Mothibe, K. J., & Chen, W. X. (2012). Production of silver carp bone powder using superfine grinding technology: Suitable production parameters and its properties. *Journal of Food Engineering*, *109*, 730–735. https://doi.org/10.1016/j.jfoodeng.2011.11.013

Wu, X., Chan, S. W., Ma, J., Li, P., Shaw, P. C., & Lin, G. (2018). Investigation of association of chemical profiles with the tracheobronchial relaxant activity of Chinese medicinal herb Beimu derived from various *Fritillaria* species. *Journal of Ethnopharmacology*, *210*, 39–46. https://doi.org/10.1016/j.jep.2017.08.027

Xiao, W., Zhang, Y., Fan, C., & Han, L. (2017). A method for producing superfine black tea powder with enhanced infusion and dispersion property. *Food Chemistry*, *214*, 242–247. https://doi.org/10.1016/j.foodchem.2016.07.096

Xie, X., Liu, Q., & Cui, S. W. (2006). Studies on the granular structure of resistant starches (type 4) from normal, high amylose and waxy corn starch citrates. *Food Research International*, *39*, 332–341. https://doi.org/10.1016/j.foodres.2005.08.004

Yang, F. G., Liu, X. N., Yang, K. J., & Cao, S. Y. (2009). Study on the angle of repose of nonuniform sediment. *Journal of Hydrodynamics*, *21*, 685–691. https://doi.org/10.1016/S1001-6058(08)60200-0

Yang, Y., Zhang, Z., Li, S., Ye, X., Li, X., & He, K. (2014). Synergy effects of herb extracts: Pharmacokinetics and pharmacodynamic basis. *Fitoterapia*, *92*, 133–147. https://doi.org/10.1016/j.fitote.2013.10.010

Yu, J., Romeo, M. C., Cavallaro, A. A., & Chan, H. K. (2018). Protective effect of sodium stearate on the moisture-induced deterioration of hygroscopic spray-dried powders. *International Journal of Pharmaceutics*, *541*, 11–18. https://doi.org/10.1016/j.ijpharm.2018.02.018

Zhang, K., Dai, Y., Hou, H., Li, X., Dong, H., Wang, W., & Zhang, H. (2018). Preparation of high quality starch acetate under grinding and its influence mechanism. *International Journal of Biological Macromolecules*, *120*, 2026–2034. https://doi.org/10.1016/j.ijbiomac.2018.09.196

Zhang, K., Dai, Y., Hou, H., Li, X., Dong, H., Wang, W., & Zhang, H. (2019). Influences of grinding on structures and properties of mung bean starch and quality of acetylated starch. *Food Chemistry*, *294*, 285–292. https://doi.org/10.1016/j.foodchem.2019.05.055

Zhang, M., Zhang, C. J., & Shrestha, S. (2005). Study on the preparation technology of superfine ground powder of *Agrocybe chaxingu* Huang. *Journal of Food Engineering*, *67*, 333–337. https://doi.org/10.1016/j.jfoodeng.2004.04.036

Zhao, G., Liang, X., Wang, C., Liao, Z., Xiong, Z., & Li, Z. (2014). Effect of superfine pulverization on physicochemical and medicinal properties of Qili powder. *Revista Brasileira de Farmacognosia-Brazilian Journal of Pharmacognosy*, *24*, 584–590. https://doi.org/10.1016/j.bjp.2014.09.006

Zhao, X., Chen, J., Chen, F., Wang, X., Zhu, Q., & Ao, Q. (2013). Surface characterization of corn stalk superfine powder studied by FTIR and XRD. *Colloids and Surfaces B: Biointerfaces*, *104*, 207–212. https://doi.org/10.1016/j.colsurfb.2012.12.003

Zhao, X., Du, F., Zhu, Q., Qiu, D., Yin, W., & Ao, Q. (2010). Effect of superfine pulverization on properties of *Astragalus membranaceus* powder. *Powder Technology*, *203*, 620–625. https://doi.org/10.1016/j.powtec.2010.06.029

Zhao, X., Yang, Z., Gai, G., & Yang, Y. (2009). Effect of superfine grinding on properties of ginger powder. *Journal of Food Engineering*, *91*, 217–222. https://doi.org/10.1016/j.jfoodeng.2008.08.024

Zhao, X., Zhu, H., Zhang, G., & Tang, W. (2015). Effect of superfine grinding on the physicochemical properties and antioxidant activity of red grape pomace powders. *Powder Technology*, *286*, 838–844. https://doi.org/10.1016/j.powtec.2015.09.025

Zheng, Y., Fu, Z., Li, D., & Wu, M. (2018). Effects of ball milling processes on the microstructure and rheological properties of microcrystalline cellulose as a sustainable polymer additive. *Materials*, *11*, 1057. https://doi.org/10.3390/ma11071057

Zhou, J. L., Li, P., Li, H. J., Jiang, Y., Ren, M. T., & Liu, Y. (2008). Development and validation of a liquid chromatography/electrospray ionization time-of-flight mass spectrometry method for relative and absolute quantification of steroidal alkaloids in *Fritillaria* species. *Journal of Chromatography A*, *1177*(1), 126–137. https://doi.org/10.1016/j.chroma.2007.11.030

Zhou, M., Ma, X., Ding, G., Wang, Z., Dan, L., Tong, Y., … Bai, G. (2017). Comparison and evaluation of antimuscarinic and anti-inflammatory effects of five *Bulbus fritillariae* species based on UPLC-Q/TOF integrated dual-luciferase reporter assay, PCA and ANN analysis. *Journal of Chromatography B*, *1041–1042*, 60–69. https://doi.org/10.1016/j.jchromb.2016.12.012

Zhou, N., Guo, D. Q., Shen, L., Chen, Q. Y., & Qin, Y. (2014). Comparative contents of four alkaloids in bulbs of *Fritillaria taipaiensis* and *Fritillaria unibracteata*. *Food Science*, *35*(12), 133–136.

Zobel, H. F. (1988). Molecules to granules: A comprehensive starch review. *Starch*, *40*, 44–50. https://doi.org/10.1002/star.19880400203

SUPPORTING INFORMATION

Additional supporting information may be found online in the Supporting Information section at the end of the article.

How to cite this article: Li C, Liu Y, Feng H, Ma S. Effect of superfine grinding on the physicochemical properties of bulbs of *Fritillaria unibracteata* Hsiao et K.C. Hsia powder. *Food Sci Nutr*. 2019;7:3527–3537. https://doi.org/10.1002/fsn3.1203